Journal of Applied Polymer Science

Fluorescence turn-on chemical sensor based on water-soluble conjugated polymer/single-walled carbon nanotube composite

Naoya Adachi, Mari Okada, Masafumi Sugeno, Takayuki Norioka
Division of Science, School of Science and Engineering, Tokyo Denki University, Hatoyama, Hiki-Gun, Saitama 350-0394, Japan
Correspondence to: N. Adachi (E-mail: nadachi@mail.dendai.ac.jp)

ABSTRACT: A chemical sensor for methyl viologen (MV^{2+}), based on a water-soluble conjugated polymer/single-walled carbon-nanotube (SWNT) composite, was fabricated. Water-soluble poly(*m*-phenylene ethynylene) with sulfonic acid side-chain groups (*m*PPE-SO_3) was synthesized via a Pd-catalyzed Sonogashira coupling reaction and used to prepare a highly stable *m*PPE-SO_3/SWNT composite with strong π–π interactions in water. The relationship between the optical properties and sensing capability of the *m*PPE-SO_3/SWNT composite in aqueous solution was investigated. The addition of MV^{2+} enhanced the fluorescence intensity of the *m*PPE-SO_3/SWNT composite by inducing a conformational change of the polymer from a helical to a random-coil structure. The water-soluble *m*PPE-SO_3/SWNT composite enabled highly sensitive fluorescence detection of MV^{2+} in aqueous solutions with no precipitation resulting from reaggregation of the SWNTs. This *m*PPE-SO_3/SWNT composite sensor system is therefore an effective turn-on chemical sensor for MV^{2+}. © 2016 Wiley Periodicals, Inc. J. Appl. Polym. Sci. **2016**, *133*, 43301.

KEYWORDS: composites; conducting polymers; graphene and fullerenes; nanotubes; optical properties; photochemistry

Received 22 June 2015; accepted 1 December 2015
DOI: 10.1002/app.43301

INTRODUCTION

Conjugated polymers with high fluorescence and electroconductive properties are photo- and electro-luminescent, and fluorescence sensor materials.[1,2] The properties of conjugated polymers can be controlled by varying their main- and side-chain structures.[3–6] In particular, poly(phenylene ethynylene) (PPE) have been widely studied because of their potential applications and their optical and electronic properties; *para*-, *meta*-, and *ortho*-linked PPE (*p*PPE, *m*PPE, and *o*PPE, respectively) have been reported.[7–12] The intermolecular π–π interactions in these PPEs can be controlled via the introduction of side chains, and control of these interactions in PPEs results in changes in their optical and electronic properties, and conformations.[9,13] Control of the π–π interactions in *m*PPE with amphiphilic or water-soluble side chains has been reported to induce a dynamic conformational change between random-coil and helical conformations.[9,14,15] Moore *et al.* reported the induction of a random-coil to helical conformational change in *meta*-linked oligo(phenylene ethynylene) by varying the solvent.[16] Biopolymers with helical conformation such as proteins and DNAs have catalytic, separation, and recognition properties.[17–20] Thus, the synthesis of helical polymers is a topic of considerable interest because of their unique properties. Huang *et al.* reported highly sensitive chemical sensing of DNA by helical *m*PPE.[15] PPEs with water-soluble side chains have been used as chemical sensors for the detection of biological and organic molecules, metal ions, and gases through changes in the fluorescence properties of the PPE.[5,6,21,22] Chemical sensors based on PPEs can also be used for the visual detection of target molecules via variations in the fluorescence properties between fluorescence on and off states.[5,6] Highly sensitive and selective chemical sensors based on water-soluble *m*PPE are currently under development.

Single-walled carbon nanotubes (SWNTs) have been extensively investigated, because of their unusual optical and electrical properties.[23,24] SWNTs are expected to be used in constructing future nanodevices for their properties such as ultra-lightweight, high mechanical strength, and a high elastic modulus.[25–29] However, the strong π–π interactions between SWNTs lead to the formation of insoluble bundle structures, and the poor solubility of the aggregated bundled SWNTs has limited their practical applications. Consequently, numerous studies have recently focused on improving the solubility of SWNTs.[30] Noncovalent functionalization of the sidewalls of SWNTs via π–π or van der Waals interactions with organic molecules affects the chemical and physical properties of SWNTs. Noncovalent functionalization can be achieved in either hydrophilic or hydrophobic adsorption dispersion media.[31,32] Noncovalent functionalizations of SWNTs using biopolymers, surfactants, small aromatic

Additional Supporting Information may be found in the online version of this article.

molecules, and π-conjugated oligomers, and polymers have been investigated.[33–38]

The functionalization of SWNTs via noncovalent wrapping using π-conjugated polymers with numerous π-electrons is a particularly interesting approach. SWNTs and conjugated polymer composites have been used in light-emitting diodes, solar cells, and chemical sensors.[39–41] We previously reported the fabrication of a water-soluble *p*PPE/SWNT composite by noncovalent functionalization in water, and investigation of the anisotropic electronic conductivity of a *p*PPE/SWNT composite film.[42] Chemical sensors based on SWNT/polymer composites are effective for detection of target molecules by adsorption on and desorption from SWNTs, with concomitant changes in the fluorescence properties of the polymer.[43] Therefore, we also investigated high fluorescence water-soluble *m*PPEs as a dispersant for SWNTs in water for sensing methyl viologen (MV^{2+}). MV^{2+} serves as an electron acceptor in photochemical and electrochemical reactions; therefore, MV^{2+} is an important molecule with potential applications in artificial photosynthesis and fuel cells. However, the use of MV^{2+} has attracted considerable attention because of its high toxicity and association with Parkinson's disease. Highly sensitive chemical sensors for MV^{2+} detection are therefore needed. Water-soluble *m*PPEs with sulfonic side chains were synthesized and used to stabilize and modify SWNTs through π–π interactions between the *m*PPE backbone and SWNT sidewalls in water. Photoinduced energy transfer from conjugated polymers to SWNTs in conjugated polymer/SWNT composites has been reported to result in effective quenching of the fluorescence emissions of the conjugated polymers.[36,44] A helical *m*PPE/SWNT composite chemical sensor would therefore be in the fluorescence off-state, until the target molecule is adsorbed. Subsequent detection of the target molecules shows the strong fluorescence because of energy transfer from *m*PPE to target molecules. The recovery of fluorescence emission would result in the fluorescence on-state. To our knowledge, although turn-off chemical sensors based on water-soluble PPEs have been widely investigated,[5,6] turn-on chemical sensors based on water-soluble PPE/SWNT composites without SWNT precipitation, have not been reported. Here, we report a novel fluorescence turn-on type chemical sensor based on *m*PPE/SWNT composite for MV^{2+} detection without SWNT precipitation. The *m*PPE/SWNT composites without SWNT precipitation by the addition of MV^{2+} can be expected to optoelectronic materials for the novel three-component nano-composite materials with each property of conjugated polymers, SWNTs, and MV^{2+}.

EXPERIMENTAL

General

All reagents and solvents were purchased from Wako Pure Chemical Industries (Osaka, Japan), Tokyo Kasei (Tokyo, Japan), or Aldrich (Sigma–Aldrich, Saint-Louis, MO), and were of analytical grade. All solvents were distilled before use. SWNTs (SuperPureTubes^{TM}) were purchased from NanoIntegris (Menlo Park, CA). Ultrapure water (>18.2 MΩ cm^{-1}), obtained using a Milli-Q system (Merck Millipore, Darmstadt, Germany), was used for all the experiments. Column chromatography was performed using a Wakogel C-200 column. Analytical thin-layer chromatography was performed using 0.25 mm silica gel 60F-coated aluminum plates (Merck Millipore, Darmstadt, Germany) and a UV254 fluorescent indicator.

NMR spectra were recorded using a Bruker AVANCE 300 FT NMR spectrometer (Bruker Corporation, Billerica, MA), operated at 300.13 MHz for ^{1}H spectra and at 100.61 MHz for ^{13}C spectra; DMSO-d_6 was used as the solvent. Chemical shifts are reported relative to tetramethylsilane as the internal standard. FT-IR spectra were obtained using a JASCO FT/IR-4200 spectrometer (JASCO, Hachioji, Japan). UV–vis spectra were recorded using a Shimadzu UV-1700 spectrometer (Shimadzu, Tokyo, Japan). Fluorescence spectra were obtained using a JASCO FP-6200ST spectrophotometer (JASCO). Raman spectra were obtained using an Olympus IX71 microscope (Olympus, Tokyo, Japan) equipped with a Princeton Instruments SpectraPro 2300 spectrophotometer (Princeton Instruments, Trenton, NJ); the spectra were recorded at an excitation wavelength of 514 nm. All optical measurements were performed at room temperature unless otherwise stated.

Water-soluble *m*PPE-SO_3

Water-soluble *m*PPE-SO_3 was synthesized via a Pd-catalyzed Sonogashira coupling reaction.[45,46] Diiodo-substituted benzenes with sulfonic acid side chains (0.10 g, 1.54×10^{-4} mol), *m*-diethynylbenzene (19.4 mg, 1.54×10^{-4} mol), CuI (0.87 mg, 4.61×10^{-6} mol), and $Pd(PPh_3)_4$ (5.3 mg, 4.61×10^{-6} mol) were combined in distilled DMF (4 mL), distilled water (2 mL), and diisopropylamine (4 mL) under N_2. The reaction mixture was heated at 100°C for 12 h. The reaction mixture was then precipitated into mixture of diethyl ether (100 mL), acetone (80 mL), and methanol (20 mL), and the raw product was reprecipitated from diethyl ether, acetone, and methanol three times. The resulted precipitate was collected and dried at 40°C overnight to afford a light-yellow solid in 60% yield. Degree of sulfonation is 1.1.[47] Water solubility is 2.3 mg mL^{-1}. ^{1}H NMR (DMSO-d_6): $\delta = 7.61$ (br, 2H, Ph), 7.29 (s, 2H, Ph), 7.18 (s, 2H, Ph), 4.10 (br, 4H, —OCH_2—), 2.64 (br, 4H, —CH_2—), 2.02 (br, 4H, —CH_2—). ^{13}C NMR (DMSO-d_6): $\delta = 155.4$, 138.7, 131.5, 131.0, 129.5, 121.3, 118.6, 96.0, 88.1, 67.1, 46.9, 25.0, 19.1. FT-IR (KBr): 2926, 1598, 1396, 1160 cm^{-1}.

Water-soluble *m*PPE-SO_3/SWNT Composite

*m*PPE-SO_3 (1.0 mg) and SWNTs (1.0 mg) were added in water (10 mL), and the mixture was sonicated for 12 h at room temperature. The mixed solution was then centrifuged at 4000 rpm ($1250 \times g$) for 30 min. After centrifugation, the suspension was filtered through a 200 nm membrane filter and washed with excess water until the filtrate was colorless. The residue was collected and resuspended in distilled water (10 mL) via sonication for 3 h at room temperature. The *m*PPE-SO_3/SWNT composite solution was used for spectroscopic analyses and molecular recognition. The degree of functionalization is 16%.[48] TEM image of *m*PPE-SO_3/SWNT composite is shown in Supporting Information Figure S1. ^{1}H NMR (DMSO-d_6): $\delta = 7.60$ (br, 2H, Ph), 7.18 (br, 4H, Ph), 4.06 (br, 4H, —OCH_2—), 2.50 (br, 4H, —CH_2—), 2.09 (br, 4H, —CH_2—). Raman shift: 1592, 1385, 175 cm^{-1}. FT-IR (KBr): 2928, 1594, 1392, 1155 cm^{-1}.

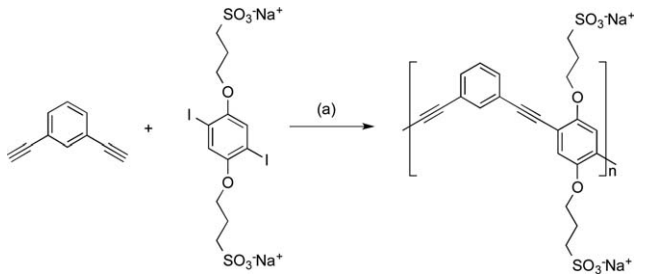

Scheme 1. Chemical Structure of Water-Soluble *m*PPE-SO_3. (a) CuI, $Pd(PPh_3)_4$, DMF, water, $^iPr_2NH$, 100°C, 12 h.

RESULTS AND DISCUSSION

Preparation of *m*PPE-SO_3/SWNT Composite

The chemical structure of *m*PPE-SO_3 with ionic side chains is shown in Scheme 1. Water-soluble *m*PPE-SO_3 was synthesized according to the reported method.[45,46] The synthesized *m*PPE-SO_3 had good solubility in both methanol and water. The formation of water-soluble conjugated polymer and SWNT composites via noncovalent functionalization was investigated in a previous study, in which water-soluble *p*PPEs with sulfonic side chains was synthesized and the formation of composites between water-soluble *p*PPEs and SWNTs in water via π–π interactions was investigated.[42] Chen *et al.* reported that *p*PPEs formed composites with SWNTs via π–π interactions in $CHCl_3$, and that *p*PPE/SWNT composite films had good electronic conductivity and mechanical strength.[49] Therefore, various conjugated polymer/SWNT composites were formed stable dispersions in various solvents. SWNTs have also been dispersed in aqueous solutions using water-soluble conjugated polymers. The PPE backbone structure was selected for composite formation with SWNTs because it is known to have strong π–π interactions, and ionic side chains were introduced to enhance the water solubility. A water-soluble *m*PPE-SO_3/SWNT composite was prepared via bath sonication, followed by centrifugation and filtration. Raman spectroscopic analysis of the dried *m*PPE-SO_3/SWNT composite showed a band attributed to the radial breathing mode at 175 cm^{-1}, a strong graphite band (G-band) at 1592 cm^{-1}, and a weak disorder band (D-band) at 1385 cm^{-1} (Supporting Information Figure S2). The ratio of the intensities of the G- and D-bands in the Raman spectrum of the *m*PPE-SO_3/SWNT composite was <0.15. The D-band is associated with defects and curvature in the CNT lattice.[50,51] A low D/G-band intensity ratio indicates lack of chemical and physical damage to the SWNTs and a low level of impurities in the *m*PPE-SO_3/SWNT composite. Dispersions of the *m*PPE-SO_3/SWNT composite were stable for a period of 6 months (no precipitation) at room temperature. These results indicate that the *m*PPE-SO_3 was incorporated into a stable *m*PPE-SO_3/SWNT composite by strong π–π interactions with the SWTN sidewalls.

Optical Properties of *m*PPE-SO_3 and *m*PPE-SO_3/SWNT Composite

The UV–vis and fluorescence spectra of the water-soluble *m*PPE-SO_3 in methanol and water at room temperature are shown in Figure 1. The *m*PPE-SO_3 spectrum has an absorption peak in the UV region at ~320 nm and the shoulder band at 370 nm in methanol indicates that this absorption peak arises from extended π-electronic conjugation along the *m*PPE backbone.[45] However, in the absorption spectrum in water, this absorption peaks in methanol are red shifted to 325 and 390 nm, respectively. The lower intensity and red shift of the absorption peak are believed to be caused by π–π interactions involved in formation of the helical conformation.[9,45] Schanze *et al.* reported that *meta*-linked PPE with sulfonic side chains undergoes a conformational transition from a random-coil to a helical structure when the solvent composition is changed.[45] The solvent-induced random-coil to helix transition of *m*PPE-SO_3 was confirmed by fluorescence measurements under different conditions in methanol and water [Figure 1(b)]. The fluorescence spectrum of *m*PPE-SO_3 in methanol shows a single peak at 405 nm due to *m*PPE backbone. This fluorescence emission peak in the visible region is characteristic of a localized excited state, which is attributed to random-coil conformation.[9] However, the fluorescence peak of *m*PPE-SO_3 in water is quenched and red shifted from 405 to 480 nm compared with that of *m*PPE-SO_3 in methanol. This fluorescence quenching and red shifting in water indicates an excimer-like emission, which probably arises from π–π stacking interactions of

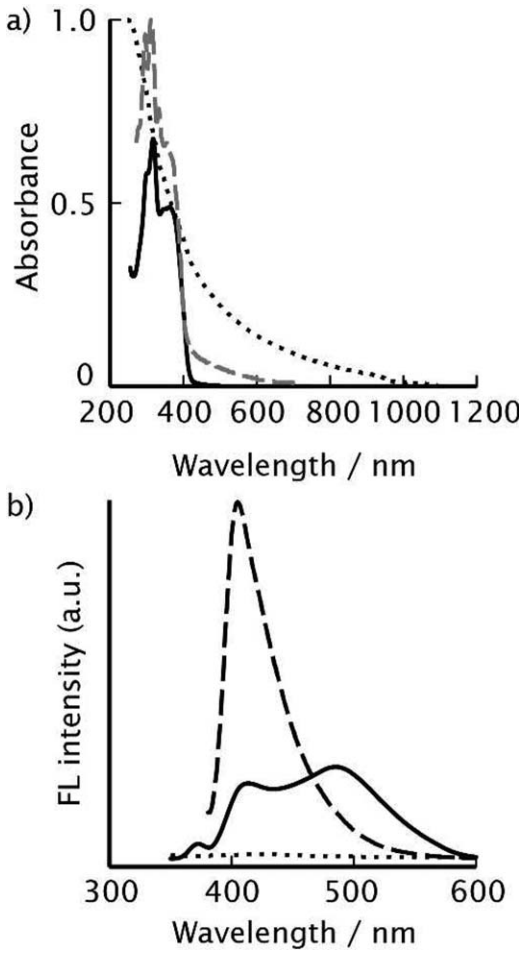

Figure 1. (a) UV–vis and (b) fluorescence spectra of water-soluble *m*PPE-SO_3 (dashed line: in methanol; solid line: in water) and *m*PPE-SO_3/SWNT composite (dotted line: in water).

phenylene ethynylene rings in the helical conformation.[9,45] The solvent-induced changes in the fluorescence emission properties of *m*PPE-SO_3 are similar to those observed for the conformational change of *m*OPE from a random-coil to a helix, as reported by Schanze *et al.*[45] These results suggest that the synthesized water-soluble *m*PPE-SO_3 undergoes a solvent-induced transition from the random-coil to the helical conformation.

Figure 1 also shows the UV–vis and fluorescence spectra of the *m*PPE-SO_3/SWNT composite in water. The *m*PPE-SO_3/SWNT dispersion shows a broad absorption band at 220–1100 nm, together with a broad absorption band at ~320 nm from *m*PPE-SO_3 adsorbed on the SWNTs.[36] The scattering of the absorption band in the *m*PPE-SO_3/SWNT composite spectrum is attributable to the presence of SWNTs in the dispersion.[24,52] In contrast, the fluorescence spectrum of the *m*PPE-SO_3/SWNT composite is significantly quenched compared with that of only *m*PPE-SO_3. This fluorescence quenching of the *m*PPE-SO_3/SWNT composite is believed to be caused by intermolecular energy transfer from the PPE backbone as an energy donor to the SWNTs as an energy acceptor.[36] These results indicate that the *m*PPE-SO_3/SWNT composite involves strong π–π interactions between the water-soluble *m*PPE-SO_3 and the SWNTs in water.

MV^{2+} Sensing by Water-soluble *m*PPE-SO_3

The ability of water-soluble *m*PPE-SO_3 to sense MV^{2+} in aqueous solutions at room temperature was investigated. Figure 2(a) shows the fluorescence spectral changes of water-soluble *m*PPE-SO_3 in water on titration with MV^{2+}. The fluorescence intensity at 405 nm gradually decreased with addition of MV^{2+}, and the fluorescence of random-coil *m*PPE-SO_3 was significantly quenched by ~80% when the concentration of added MV^{2+} in the *m*PPE-SO_3 aqueous solution reached 10 μM. The fluorescence intensity at 480 nm which is attributed to the helical conformation, was significantly quenched by the addition of MV^{2+} (3.0 μM). These results indicate that the fluorescence quenching after addition of MV^{2+} is caused by electron or energy transfer from the conjugated *m*PPE backbone to MV^{2+}, and that the water-soluble *m*PPE-SO_3 is strongly bound to MV^{2+} via electrostatic attraction. And then, the MV^{2+} was changed to MV^{+} by the obtained energy at the energy transfer from *m*PPE-SO_3. The fluorescence quenching at 480 nm suggests that a conformational change from the helical to the random-coil structure is induced by the addition of MV^{2+}. The relative fluorescence intensities at 405 and 480 nm were evaluated as a function of MV^{2+} concentration. Specifically, the fluorescence quenching of *m*PPE-SO_3 was determined using the Stern–Volmer equation $[(F_0/F = K_{SV}[MV^{2+}] + 1)$, where F_0 and F are the steady-state fluorescence intensities in the absence and presence of MV^{2+}, respectively, K_{SV} is the Stern–Volmer quenching constant (M^{-1}), and $[MV^{2+}]$ is the MV^{2+} concentration. The Stern–Volmer plots for *m*PPE-SO_3 are shown in Figure 2(b). The figure shows that highly efficient fluorescence quenching occurred even at low MV^{2+} concentrations. The initial slope of the Stern–Volmer plot provided the Stern–Volmer constants $K_{SV} = 2.6 \times 10^5\ M^{-1}$ at 405 nm and $K_{SV} = 2.0 \times 10^6\ M^{-1}$ at 480 nm ($[MV^{2+}] = 10\ \mu M$). This high K_{SV} value at 480 nm is the result of high delocalization of singlet excitons and the rapidity of energy migration along the conjugated backbone of *m*PPE-SO_3; this K_{SV} value is similar to those for the addition of MV^{2+} to water-soluble PPEs. The detection limit of MV^{2+} was determined to be 1.0 μM from the Stern–Volmer plots.

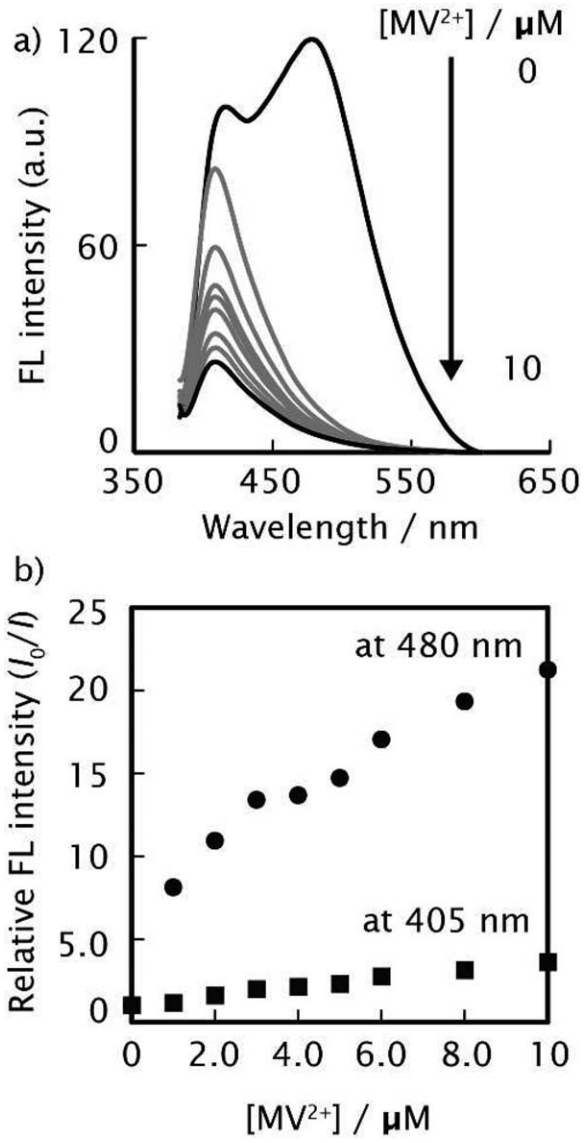

Figure 2. (a) Changes in fluorescence spectrum of water-soluble *m*PPE-SO_3 in water on addition of different concentrations of MV^{2+} (0, 1.0, 3.0, 5.0, 7.0 9.0, and 10.0 μ*M*) and (b) Stern–Volmer plots for fluorescence quenching of *m*PPE-SO_3 in presence of different concentrations of MV^{2+} (0, 1.0, 3.0, 5.0, 7.0 9.0, and 10.0 μ*M*) at 405 (■) and 480 (●) nm.

MV^{2+}-sensing Capability of *m*PPE-SO_3/SWNT Composite

The fluorescence emission properties of the *m*PPE-SO_3/SWNT composite solution were also sensitive to the presence of MV^{2+}. Figure 3(a) shows the changes in the fluorescence spectrum of the *m*PPE-SO_3/SWNT composite in water on titration with MV^{2+}. Specifically, the fluorescence intensity of the *m*PPE-SO_3/SWNT composite at 405 nm increased about 90-hold by the addition of MV^{2+} until 1.0 μM. The fluorescence intensity then gradually decreased when the MV^{2+} concentration was increased from 1.0 to 10 μM [Figure 3(b)]. The K_{SV} value in

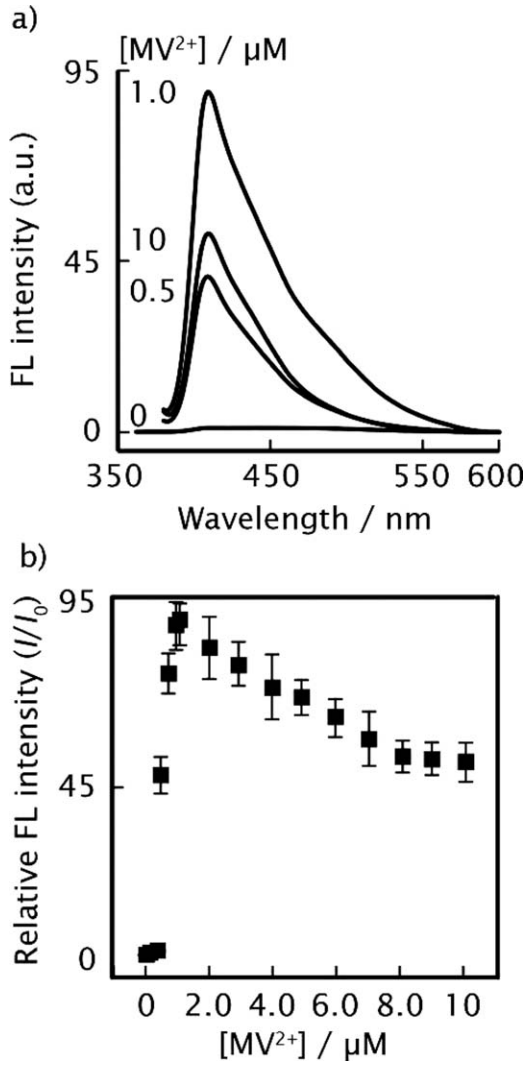

Figure 3. (a) Changes in fluorescence spectrum of water-soluble *m*PPE-SO_3/SWNT in water on titration with MV^{2+} (0, 0.5, 1.0, and 10.0 μ*M*) and (b) changes in fluorescence intensity of *m*PPE-SO_3/SWNTs in presence of different concentrations of MV^{2+} (0, 0.1, 0.3, 0.5, 0.9, 1.0, 2.0, 3.0, 4.0, 5.0, 6.0, 7.0, 8.0, 9.0, and 10.0 μ*M*) at 405 nm (■).

the fluorescence decreased range of MV^{2+} concentrations between 1.0 and 10 μM was 7.2×10^4 M^{-1} at 405 nm ($[MV^{2+}] = 10$ μM). The detection limit of MV^{2+} was determined to be 500 nM from titration curves. The detection limit and K_{SV} value suggests that the *m*PPE-SO_3/SWNT composite compared to the only *m*PPE-SO_3 was high sensitive chemical sensor with detection limit of nM, and the MV^{2+} in the *m*PPE-SO_3/SWNT composite solution was slowly diffused for difference of K_{SV} value about 10^2 order by presence of the SWNT. The mechanism of the fluorescence change is considered to be as follows. The fluorescence emission of the *m*PPE-SO_3/SWNT composite increases for changes of energy transfer through electrostatic interactions from the energy transfer between *m*PPE-SO_3 and SWNT to the energy transfer between *m*PPE-SO_3 and MV^{2+}, when the concentration of added MV^{2+} is <1.0 μM. The fluorescence intensity is then gradually quenched because of greater energy transfer from *m*PPE-SO_3 to MV^{2+} on addition of MV^{2+} at concentrations >1.0 μM. Additionally, the MV^{2+} was reduced to MV^{+} by using the obtained energy due to the energy transfer from *m*PPE-SO_3 to the MV^{2+}. These results indicate that the *m*PPE-SO_3/SWNT composite in aqueous solution acts as a highly sensitive turn-on chemical sensor for MV^{2+} detection. Typically, chemical sensors fabricated using polymer/CNT composites form precipitates as a result of reaggregation of desorbed CNTs on recognition of target molecules.[43,53] However, the SWNTs in the *m*PPE-SO_3/SWNT composite were not precipitated on recognition of the target MV^{2+} [Figure 4(a)]. Dispersions of the *m*PPE-SO_3/SWNT composite formed on addition of MV^{2+} were stable for longer than 1 month at room temperature. The UV–vis absorption spectrum of an *m*PPE-SO_3/SWNT composite aqueous solution containing 10 μM MV^{2+} was collected to confirm the dispersion state of the *m*PPE-SO_3/SWNT composite [Figure 4(b)]. Figure 4(b) shows the UV–vis absorption spectrum of the water-soluble *m*PPE-SO_3/SWNT composite solution containing 10 μM MV^{2+}. The spectrum of the *m*PPE-SO_3/SWNT composite with

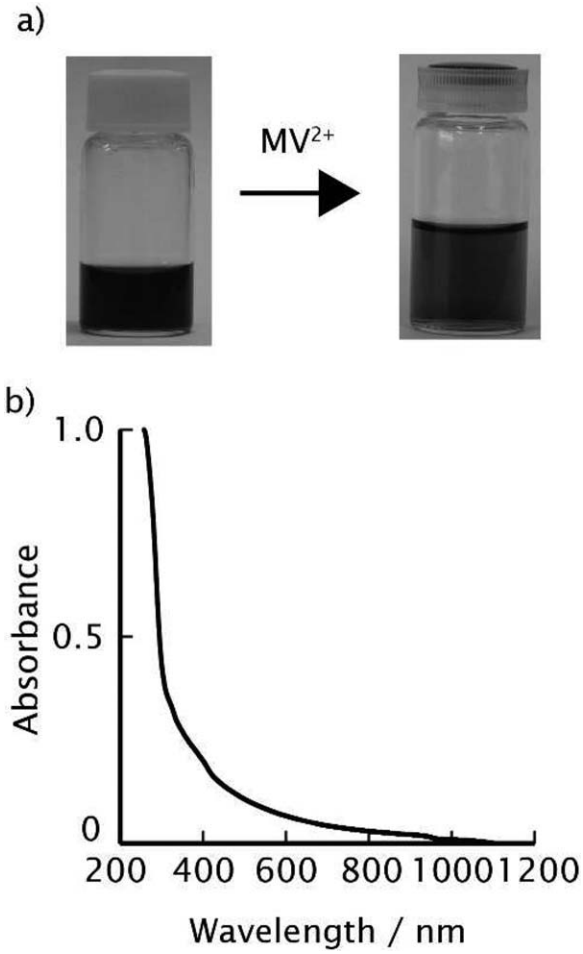

Figure 4. (a) Photographs of *m*PPE-SO_3/SWNT composite (left) and *m*PPE-SO_3/SWNT composite addition of 10 μM MV^{2+} (right) in water. (b) UV–vis spectrum of water-soluble *m*PPE-SO_3/SWNT composite in water after addition of 10 μM MV^{2+}.

MV^{2+} showed scattering of the broad absorption band from 220 to 1100 nm; absorption peaks at 320 and 370 nm from *m*PPE-SO_3 were not observed. FT-IR spectrum was characterized using the *m*PPE-SO_3/SWNT composite with MV^{2+} (Supporting Information Figure S3). The FT-IR spectrum of *m*PPE-SO_3/SWNT composite with MV^{2+} shows due to pyridine rings and sulfonic acid groups of *m*PPE-SO_3 at 1642 and 1338 cm^{-1}, respectively.[47,54] The FT-IR spectrum of *m*PPE-SO_3/SWNT composite with MV^{2+} differs from the FT-IR spectrum of *m*PPE-SO_3/SWNT composite. The intensity of typical $-SO_3^-$ bands at 1384 cm^{-1} was decreased, and this peak was shifted to the lower wavenumbers at 1338 cm^{-1}. The changes of FT-IR peak suggest that there are effect on the interactions between sulfonic acid groups of *m*PPE-SO_3 and MV^{2+}. The photograph and UV–vis absorption spectrum in Figure 4 indicate that the SWNTs were in a stably dispersed state in aqueous solution. This ability to maintain stable dispersion during MV^{2+} sensing is speculated to be a consequence of the strong π–π interactions between the hydrophobic PPE backbone and the hydrophobic SWNTs in water. We recorded the UV–vis and fluorescence spectra of the *m*PPE-SO_3/SWNT composite after addition of Cu^{2+} to verify that the stable dispersion was not a consequence of π–π interactions between the SWNTs and MV^{2+} (Supporting Information Figure S4). The UV–vis and the fluorescence spectra of the *m*PPE-SO_3/SWNT composite in the presence of added Cu^{2+} also showed a broad absorption band and a fluorescence peak at 405 nm; precipitates resulting from reaggregation of the SWNTs were not observed. These results suggest that the *m*PPE-SO_3/SWNT composite in water is highly sensitive chemical sensors for MV^{2+} detection, and that this *m*PPE-SO_3/SWNT composite sensor system has potential applications in future turn-on chemical sensors.

CONCLUSIONS

We fabricated highly sensitive chemical sensors consisting of *m*PPE-SO_3 and an *m*PPE-SO_3/SWNT composite for MV^{2+} detection. Water-soluble *m*PPE-SO_3 was synthesized by a Sonogashira cross-coupling reaction. The *m*PPE-SO_3 and *m*PPE-SO_3/SWNT composite sensor systems both detected MV^{2+} at micro- and nanomolar concentrations. The *m*PPE-SO_3 functions as a fluorescence turn-off chemical sensor, in which fluorescence quenching caused by energy transfer from the PPE backbone to MV^{2+} serves as the indicator for MV^{2+} detection. The *m*PPE-SO_3/SWNT composite was formed via π–π interactions between the *m*PPE and the SWNTs in aqueous solution. The *m*PPE-SO_3/SWNT composite is a turn-on sensor material, with high MV^{2+} sensitivity. The construction of these modified conjugated polymers and the *m*PPE-SO_3/SWNT composite is important for the development of novel composite chemical sensors with high sensitivities. Such highly sensitive chemical sensors may be applicable to monitoring of MV^{2+} in the environment. Additionally, the *m*PPE-SO_3/SWNT composite without SWNTs precipitation by the addition of MV^{2+} was expected to solar cells for effective photoindeuced energy transfer properties between *m*PPE-SO_3/SWNT composite and MV^{2+}.

ACKNOWLEDGMENTS

This work was partly supported by the Research Institute for Science and Technology of Tokyo Denki University, Japan, Grant Number Q15K-04.

REFERENCES

1. Skotheim, T. A.; Reynolds, J. Handbook of Conducting Polymers, 3rd ed.; CRC Press: New York, **2007**.
2. Friend, R. H.; Gymer, R. W.; Holmes, A. B.; Burroghes, J. H.; Marks, R. N.; Taliani, C.; Bradley, D. D. C.; Dos Stantos, D. A.; Brédas, J. L.; Lögdlund, M.; Salaneck, W. R. *Nature* **1999**, *397*, 121.
3. Bunz, U. H. F. *Chem. Rev.* **2000**, *100*, 1605.
4. Jiang, H.; Taranekar, P.; Reynolds, J. R.; Schanze, K. S. *Angew. Chem. Int. Ed.* **2009**, *48*, 4300.
5. McQuade, D. T.; Pullen, A. E.; Swager, T. M. *Chem. Rev.* **2000**, *100*, 2537.
6. Thomas, S. W., III; Joly, G. D.; Swager, T. M. *Chem. Rev.* **2007**, *107*, 1339.
7. Kim, J.; Swager, T. M. *Nature* **2001**, *411*, 1030.
8. Rose, A.; Zhu, Z.; Madigan, C. F.; Swager, T. M.; Bulovic, V. *Nature* **2005**, *434*, 876.
9. Price, R. B.; Saven, J. G.; Wolynes, P. G.; Moore, J. S. *J. Am. Chem. Soc.* **1999**, *121*, 3114.
10. Banno, M.; Yamaguchi, T.; Nagai, K.; Kaiser, C.; Hecht, S.; Yashima, E. *J. Am. Chem. Soc.* **2012**, *134*, 8718.
11. Peng, Z.; Pan, Y.; Xu, B.; Zhang, J. *J. Am. Chem. Soc.* **2000**, *122*, 6619.
12. Kuroda, D. G.; Singh, C. P.; Peng, Z.; Kleiman, V. *Science* **2009**, *326*, 263.
13. Sato, T.; Jiang, D. L.; Aida, T. *J. Am. Chem. Soc.* **1999**, *121*, 10658.
14. Hecht, S.; Khan, A. *Angew. Chem. Int. Ed.* **2003**, *42*, 6021.
15. Huang, Y. Q.; Fan, Q. L.; Liu, X. F.; Fu, N. N.; Huang, W. *Langmuir* **2010**, *26*, 19120.
16. Lahiri, S.; Thompson, J. L.; Moore, J. S. *J. Am. Chem. Soc.* **2000**, *122*, 11315.
17. Ito, S.; Shen, L.; Dai, Z.; Wu, S. C.; Collins, L. B.; Swenberg, J. A.; He, C.; Zhang, Y. *Science* **2011**, *333*, 1300.
18. Sancar, A. *Chem. Rev.* **2003**, *103*, 2203.
19. Jamieson, E. R.; Lippard, S. *J. Chem. Rev.* **1999**, *99*, 2467.
20. Swwman, N. C. *Nature* **2003**, *421*, 427.
21. DiCesare, N.; Pinto, M. R.; Schanze, K. S.; Lakowicz, J. R. *Langmuir* **2002**, *18*, 7785.
22. Bunz, U. H. F.; Rotello, V. M. *Angew. Chem. Int. Ed.* **2010**, *49*, 3268.
23. Odom, T. W.; Huang, J. L.; Kim, P.; Lieber, C. M. *Nature* **1998**, *391*, 62.
24. Bachilo, S. M.; Strano, M. S.; Kittrell, C.; Hauge, R. H.; Smalley, R. E.; Weisman, R. B. *Science* **2002**, *298*, 2361.
25. Salvetat-Delmotte, J. P.; Rubio, A. *Carbon* **2002**, *40*, 1729.

26. Duclaux, L. *Carbon* **2002**, *40*, 1751.
27. Hierold, C.; Jungen, A.; Stampfer, C.; Helbling, T. *Sens. Actuat. A* **2007**, *136*, 51.
28. Schnorr, J. M.; Swager, T. M. *Chem. Mater.* **2011**, *23*, 646.
29. De Volder, M. F. L.; Tawfick, S. H.; Baughman, R. H.; Hart, A. *J. Sci.* **2013**, *339*, 535.
30. Tasis, D.; Tagmatarchis, N.; Bianco, A.; Prato, M. *Chem. Rev.* **2006**, *106*, 1105.
31. Li, Q.; Zhang, J.; Yan, H.; He, M.; Liu, Z. *Carbon* **2004**, *42*, 287.
32. Bartelmess, J.; Ballesteros, B.; de la Torre, G.; Kiessling, D.; Campidelli, S.; Prato, M.; Torres, T.; Guldi, D. M. *J. Am. Chem. Soc.* **2010**, *132*, 16202.
33. Tu, X.; Manohar, S.; Jagota, A.; Zheng, M. *Nature* **2009**, *460*, 250.
34. Moore, V. C.; Strano, M. S.; Haroz, E. H.; Hauge, R. H.; Smalley, R. E. *Nano Lett.* **2003**, *3*, 1379.
35. Tomonari, Y.; Murakami, H.; Nakashima, N. *Chem. Eur. J.* **2006**, *12*, 4027.
36. Chen, J.; Liu, H.; Weimer, W. A.; Halls, M. D.; Waldeck, D. H.; Walker, G. C. *J. Am. Chem. Soc.* **2002**, *124*, 9034.
37. Li, X.; Zhang, L.; Wang, X.; Shimoyama, I.; Sun, X.; Seo, W. S.; Dai, H. *J. Am. Chem. Soc.* **2007**, *129*, 4890.
38. Zhang, Z.; Che, Y.; Smaldone, R. A.; Xu, M.; Bunes, B. R.; Moore, J. S.; Zang, L. *J. Am. Chem. Soc.* **2010**, *132*, 14113.
39. Bhattacharyya, S.; Kymakis, E.; Amaratunga, G. A. *J. Chem. Mater.* **2004**, *16*, 4819.
40. Xu, Z.; Hu, B.; Ivanov, I. N.; Geohegan, D. B. *Appl. Phys. Lett.* **2005**, *87*, 263118.
41. Pang, X.; Imin, P.; Zhitomirsky, I.; Adronov, A. *Macromolecules* **2010**, *43*, 10376.
42. Adachi, N.; Fukawa, T.; Tatewaki, Y.; Shirai, H.; Kimura, M. *Macromol. Rapid Commun.* **2008**, *29*, 1877.
43. Zhao, C.; Qu, K.; Song, Y.; Xu, C.; Ren, J.; Qu, X. *Chem. Eur. J.* **2010**, *16*, 8147.
44. Cheng, F.; Imin, P.; Maunders, C.; Botton, G.; Andronov, A. *Macromolecules* **2008**, *41*, 2304.
45. Tan, C.; Pinto, M. R.; Kose, E.; Ghiviriga, I.; Schanze, K. S. *Adv. Mater.* **2004**, *16*, 1208.
46. Tan, C.; Pinto, M. R.; Schanze, K. S. *Chem. Commun.* **2002**, 446.
47. Tsai, H. S.; Wang, Y. Z.; Lin, J.-J.; Lien, W. F. *J. Appl. Polym. Sci.* **2010**, *116*, 1686.
48. Hu, H.; Zhao, B.; Hamon, M. A.; Kamaras, K.; Itkis, M. E.; Haddon, R. C. *J. Am. Chem. Soc.* **2003**, *125*, 14893.
49. Chen, J.; Ramasubramaniam, R.; Xue, C.; Liu, H. *Adv. Funct. Mater.* **2006**, *16*, 114.
50. Rao, A. M.; Richter, E.; Bandow, S.; Chase, B.; Eklund, P. C.; Williams, K. A.; Fang, S.; Subbaswamy, K. R.; Menon, M.; Thess, A.; Smalley, R. E.; Dresselhaus, G.; Dresselhaus, M. S. *Science* **1997**, *275*, 187.
51. Rao, A. M.; Chen, J.; Richter, E.; Eklund, P. C.; Haddon, R. C.; Venkateswaran, U. D.; Kwon, Y. K.; Tománek, D. *Phys. Rev. Lett.* **2001**, *86*, 3895.
52. Maeda, Y.; Kimura, S.; Kanda, M.; Hirashima, Y.; Hasegawa, T.; Wakahata, T.; Lian, Y.; Nakahodo, T.; Tsuchiya, T.; Asakusa, T.; Lu, J.; Zhang, X.; Gao, Z.; Yu, Y.; Nagase, S.; Kazaoui, S.; Minami, N.; Shimizu, T.; Tokumoto, H.; Saito, R. *J. Am. Chem. Soc.* **2005**, *127*, 10287.
53. Zhang, L.; Li, T.; Li, B.; Li, J.; Wang, E. *Chem. Commun.* **2010**, *46*, 1476.
54. Kondo, M.; Miyake, J.; Tada, K.; Kawatsuki, N. *Chem. Lett.* **2011**, *40*, 264.